

Growth and characterization of minute $\text{BaFe}_{12-2x}\text{Ti}_x\text{Co}_x\text{O}_{19}$ crystals from high-temperature solution

Koichi Watanabe* and Junko Kawabe

Department of Materials Chemistry, Faculty of Engineering, Gunma University, Kiryu, Gunma 376, Japan

Minute crystals of barium hexaferrite containing small amounts of Ti^{4+} and Co^{2+} ions have been prepared by the slow cooling method from a high-temperature solution of the $\text{Na}_2\text{O}-\text{B}_2\text{O}_3$ system. Magnetic properties (coercivity, saturation magnetization, remanence) and lattice parameters were measured as a function of Ti^{4+} and Co^{2+} concentration in the crystals. The site preferences for Ti^{4+} and Co^{2+} ions are also discussed.

Barium hexaferrite, $\text{BaFe}_{12}\text{O}_{19}$, belongs to the hexagonal system ($P6_3/mmc$) and has a ferromagnetic character and a high magnetic anisotropy with the easy axis parallel to the c -axis. Perpendicular recording using barium ferrite particulate media has been widely investigated since it is found to have advantages in high density recording and high productivity for magnetic tape and floppy disk applications.^{1,2} In addition, other advantages are their excellent high-density recording performances, their resistance to oxidation or corrosion, and the fact that they preserve the existing head-medium interface. Moreover, small amounts of Ti^{4+} and Co^{2+} ions substituted for Fe^{3+} in barium ferrite can reduce appreciably the coercivity and magnetic anisotropy without significantly affecting the saturation magnetization.³ This is also an advantage for recording media. Minute single $\text{BaFe}_{12}\text{O}_{19}$ crystals containing small amounts of Ti^{4+} and Co^{2+} ions and consisting of particles in the μm range are necessary to accomplish this. Nowadays, such materials are prepared industrially by the glass crystallization method, which includes the complex processes of rapid solidification, recrystallization at high temperatures, and dissolution and removal of the glass matrix using an organic acid compound.^{4,5} In the glass-ceramics field, it was well known that a small amount of TiO_2 in a glass matrix plays an important role as a nucleating agent and accelerates crystallization.⁶ The same role of TiO_2 will also be expected for the growth of barium hexaferrite crystals from high-temperature solution. In solution growth, it is generally known that there exists a metastable region adjacent to the equilibrium solubility curve in which spontaneous crystallization is improbable, in spite of the fact that the solution in this region is supersaturated. On increasing supersaturation, nucleation occurs immediately beyond this metastable region, and growth of crystals proceeds. The width of this region varies depending on the solubility, solution composition, crystallizing substance, the cooling rate of solution, viscosity, agitation, etc., as well as additives. An addition of dopant to a growth solution narrows the width of this region, leading to easier nucleation and crystal growth. Therefore, a large number of minute monosized crystals can be anticipated to instantly precipitate over a short time in a growth solution.^{7,8}

The purpose of the present study is to find the optimum conditions for the preparation of monosized minute barium hexaferrite single crystals of good quality containing small amounts of Ti^{4+} and Co^{2+} ions from a high-temperature solution of the $\text{Na}_2\text{O}-\text{B}_2\text{O}_3$ system, and to examine the effect of TiO_2 and CoO dopants upon the magnetic properties of the grown crystals.

Experimental

For the growth of minute single $\text{BaFe}_{12}\text{O}_{19}$ crystals, a mixture (mol ratio = 1:6) of BaCO_3 and Fe_2O_3 of chemical reagent

grade was used as a solute and Na_2CO_3 as a solvent. B_2O_3 (5 mass%) was used to achieve stable growth, since it has the effect of lowering the solution temperature, preventing the vaporization of the solvent and reducing the viscosity of the solution.⁹ TiO_2 and CoO in the range of 0–5 mass% relative to $\text{BaFe}_{12}\text{O}_{19}$ were used as dopants. A mixture (15 g) containing the solute, solvent and dopant in the desired ratio was packed into a 20 ml covered Pt crucible. The mixture in the crucible was maintained at 1200 °C for 20 h in a resistance-heated furnace, and cooled to 800 °C at a cooling rate of 2, 4 or 8 °C h⁻¹ and then removed from the furnace. At the end of a run, the growth solution in the crucible and the solvent adhering to the as-grown crystals was washed out using 2 M HCl. After leaching to remove solvent and other soluble phases, the size of the grown crystals was monitored using sieves and the yield (%) of each run was estimated relative to the amount of the solute used. The crystal phase was identified by wide-angle X-ray powder diffraction (XRD) using graphite-monochromated Cu-K α radiation. The chemical composition of the grown crystals was quantitatively analyzed by the inductively coupled plasma (ICP) method. Samples (0.100 g) were fused with sodium carbonate (1.000 g) in a platinum crucible for 1 h at 1000 °C, and treated with 6 M HCl. After the sample solution was diluted to 1 l with water, it was analyzed. Lattice parameters for the a - and c -axes of grown crystals were measured by a least-squares method (Rad-c system program, Rigaku Denki Co.) using XRD with elemental Si as an external standard. The external morphology of the grown crystals was observed using a scanning electron microscope (SEM) and an optical microscope. Magnetic properties, coercivity, remanence and saturation magnetization, of the grown crystals were measured at room temperature in a magnetic field of 5 kOe using a vibrating sample magnetometer (VSM) with a high purity Ni metal standard (99.99%) as reference. Ground powder particles were used to measure the magnetic anisotropy, size and shape of as-grown crystals.

Results and Discussion

As a typical example, Fig. 1 shows an SEM photograph of minute $\text{BaFe}_{12}\text{O}_{19}$ crystals grown from a solution containing 10 mass% Na_2O and 5 mass% B_2O_3 solvent with 1 mass% TiO_2 and 1 mass% CoO as dopants. All these crystals were formed in the solution, and their habit changed as crystals grew larger. The crystals obtained were confirmed to be single-phase $\text{BaFe}_{12}\text{O}_{19}$ by XRD in each case. Moreover, it was verified by both ICP and electron probe microanalysis (EPMA) that boron, sodium and platinum ions were not present in the crystals. Most of crystals are <50 μm in diameter and the average size is ca. 10 μm . As can be seen in Fig. 1, the habit of

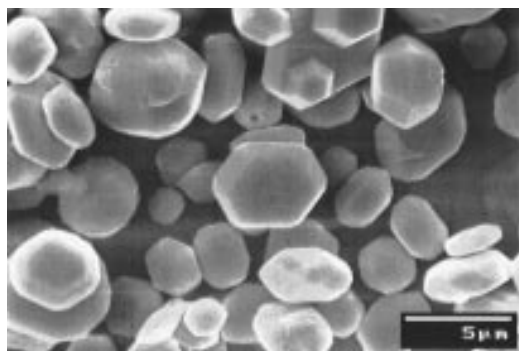


Fig. 1 SEM photograph of minute $\text{BaFe}_{12}\text{O}_{19}$ crystals formed in the growth solution containing 1 mass% TiO_2 and 1 mass% CoO . Note the evolution of the habit from hexagonal dipyramidal, that truncated by $\{0001\}$, to hexagonal tabular as crystals become larger.

grown crystals varies with the size, independent of the amount of Ti^{4+} and/or Co^{2+} ions contained in the crystals; crystals smaller than $5\ \mu\text{m}$ generally adopt a hexagonal dipyramidal habit bounded by only $\{10\bar{1}1\}$ faces and developing in the c -axial direction; for crystals between 5 and $30\ \mu\text{m}$, the $\{0001\}$ face starts to appear and the habit becomes hexagonal dipyramidal truncated by $\{0001\}$ faces; crystals larger than this size show a hexagonal tabular habit developing in the a -axial direction and bounded by $\{0001\}$ and $\{11\bar{2}0\}$ faces both showing flat surfaces. Fig. 2 illustrates the habit modification depending on the size change of $\text{BaFe}_{12}\text{O}_{19}$ crystals. Addition of TiO_2 and/or CoO into the growth solution did not have an effect upon the crystal habit, but does have a remarkable effect upon the crystal size and yield. Addition of TiO_2 or CoO diminishes the percentage total yield of crystals but increases the percentage yield of crystals smaller than $30\ \mu\text{m}$. Addition of TiO_2 in particular is very effective in leading to the formation of minute crystals. It appears that TiO_2 acts as a nucleant in the solution of the present system. It was also observed that the cooling rate did not have any significant effect upon crystal habit, size and yield.

Table 1 lists starting chemical compositions and the elemental analyses, yields and segregation coefficients of crystals

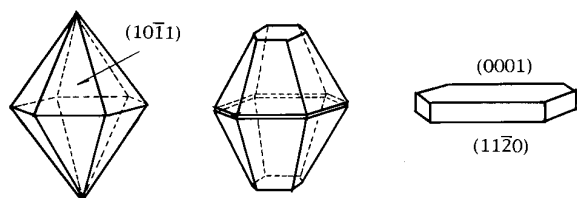


Fig. 2 Schematic drawing of the habit modification of $\text{BaFe}_{12}\text{O}_{19}$ crystals depending on a change of the size

obtained in the present study. The chemical compositions of the crystals obtained deviate widely from the stoichiometric values (Ba, 12.36 mass%; Fe, 60.29 mass%) expected for $\text{BaFe}_{12}\text{O}_{19}$. The amount of Ti^{4+} and Co^{2+} ions incorporated in the crystals increases linearly with the amount added to the solution. However, when $> 5\ \text{mass}\%$ TiO_2 and/or CoO were added to the growth solution, $\text{BaFe}_{12}\text{O}_{19}$ crystals did not form and the growth of ilmenite, FeTiO_3 , and/or other crystals was found. When the same amount of TiO_2 and CoO was added to growth solutions (run 15, 16, 25), Co^{2+} is more readily incorporated into the crystals than Ti^{4+} and the yield of crystals increased with an increase of CoO . The distribution coefficients (crystal/solution) of Ti^{4+} and Co^{2+} ions are 0.8 and 1.0, respectively. Segregation coefficients were calculated in order to determine the amounts of Ti^{4+} and Co^{2+} ions which should be incorporated into the $\text{BaFe}_{12}\text{O}_{19}$ crystals. The segregation coefficients of Ti^{4+} $[\text{Ti}/(\text{Ti} + \text{Fe})](\text{crystal})/[\text{Ti}/(\text{Ti} + \text{Fe})](\text{solution})$, and Co^{2+} $[\text{Co}/(\text{Co} + \text{Fe})](\text{crystal})/[\text{Co}/(\text{Co} + \text{Fe})](\text{solution})$, are also given in Table 1. The segregation coefficients of Ti^{4+} and Co^{2+} are observed to vary to some extent. Moreover, judging from the data of the distribution and segregation coefficients it is clear that Co^{2+} ions are more easily incorporated into the crystals than Ti^{4+} ions.

Fig. 3 and 4 show the variation of the a and c lattice parameters, respectively, with the amount of Ti^{4+} and Co^{2+} incorporated in the $\text{BaFe}_{12}\text{O}_{19}$ crystals. The lattice parameters of the grown crystals decreased slightly in both a and c directions with increased Ti^{4+} and Co^{2+} content. It is of note to consider the site preferences for Ti^{4+} and Co^{2+} ions in $\text{BaFe}_{12}\text{O}_{19}$ crystals. $\text{BaFe}_{12}\text{O}_{19}$ crystals, with a magnetoplumbite structure, consists of blocks of the cubic spinel lattice (designated S) separated by a hexagonal closed-packed block (R) containing Ba ions. Of the twelve Fe ions in the formula unit, two occupy tetrahedral sites ($4f_{IV}$) one an octahedral site ($2a$) in an S block, two ions occupy octahedral sites ($4f_{VI}$) and

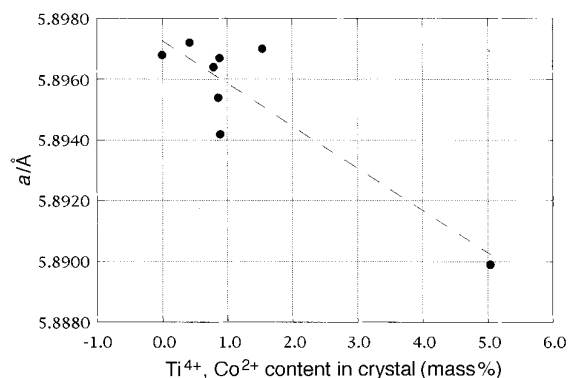


Fig. 3 Variation of the a lattice parameter depending on the Ti^{4+} and Co^{2+} content

Table 1 Starting chemical compositions, analytical values, yields and segregation coefficients; * indicates a stoichiometric chemical composition of $\text{BaFe}_{12}\text{O}_{19}$

run	chemical composition (mass%)						elemental composition (mass%)					segregation coefficient (mass%)	
	Na_2O	B_2O_3	BaO	Fe_2O_3	TiO_2	CoO	Ba	Fe	Ti	Co	yield (%)	Ti	Co
15	10.00	5.00	11.72	73.27	0.00	0.00	13.03	61.37	0.00	0.00	72.23	0.00	0.00
25	10.00	5.00	11.72	71.27	1.00	1.00	12.12	63.32	0.54	1.00	67.05	0.71	1.00
16	10.00	5.00	11.72	67.27	3.00	3.00	12.18	65.37	2.09	2.95	50.43	0.84	0.90
23	10.00	5.00	11.72	72.27	1.00	0.00	12.04	67.99	0.42	0.00	31.68	0.53	0.00
19	10.00	5.00	11.72	72.27	0.75	0.25	12.73	60.83	0.49	0.39	65.33	0.91	1.65
26	10.00	5.00	11.72	72.27	0.50	0.50	12.15	68.08	0.26	0.53	56.23	0.65	1.00
20	10.00	5.00	11.72	72.27	0.25	0.75	12.53	66.19	0.21	0.68	71.53	1.07	0.89
18	10.00	5.00	11.72	72.27	0.00	1.00	12.50	63.61	0.00	0.86	73.18	0.00	0.88
*							12.36	60.29					

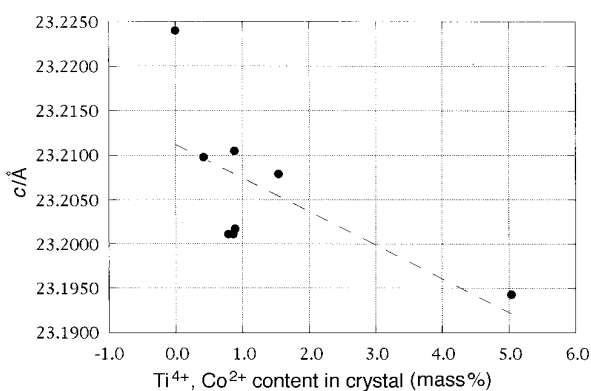


Fig. 4 Variation of the *c* lattice parameter depending on the Ti^{4+} and Co^{2+} content

one a trigonal site (2b) surrounded by five oxygen ions in an R block while six ions are in octahedral sites (12k) between S and R blocks.^{3,10} There are several papers that report the site preferences of Ti^{4+} and Co^{2+} ions.^{11–14} Recently, it was verified by Mössbauer spectroscopy that Ti^{4+} and Co^{2+} ions substitute for Fe^{3+} ions at the $4f_{\text{VI}}$ octahedral site and the 2b trigonal site in the R block;¹⁵ charge balance is achieved by the relation $\text{Co}^{2+} + \text{Ti}^{4+} = 2\text{Fe}^{3+}$. The ionic radii of Fe^{3+} and Ti^{4+} in six-fold coordination at octahedral sites are 0.79 and 0.75 Å, respectively, while the ionic radii of Co^{2+} in six- and in four-fold coordination are 0.89 and 0.68 Å, respectively.¹⁶ Therefore, if six-coordinate Co^{2+} (0.89 Å) is incorporated at a $4f_{\text{VI}}$ octahedral site in a crystal, the lattice parameters should be increased which is not observed experimentally. Accordingly, we propose that some of the Co^{2+} ions are four-coordinate (0.68 Å) and incorporated at the 2b trigonal site in R blocks.

Magnetic properties of the as-grown crystals are summarized in Table 2. It is observed that the coercivity decreases considerably with an increase of Ti^{4+} and Co^{2+} content, whereas decreases in the remanence and saturation magnetism are relatively small. In particular, an increase of Co^{2+} incorporation drastically reduced the coercivity, whereas Ti^{4+} did not give such a remarkable effect. These changes in the magnetic properties of the grown crystals are in good agreement with the results reported previously, although the measured values of coercivity are somewhat lower than in the literature.^{3,4,15}

The saturation magnetic moment, μ_s , per formula unit of $\text{BaFe}_{12}\text{O}_{19}$ is $20 \mu_{\text{B}}$, by adding the upward spin moments of Fe^{3+} ($5 \mu_{\text{B}}$, 0 K) ions at 12k, 2b and 2a sites, and subtracting the downward spin moments at $4f_{\text{IV}}$ and $4f_{\text{VI}}$ sites.^{3,17}

$$\mu_s = 5(6\mu_{12k} + \mu_{2a} + \mu_{2b} - 2\mu_{4f_{\text{IV}}} - 2\mu_{4f_{\text{VI}}}) = 20 \mu_{\text{B}} \quad (1)$$

In the present study, the largest mass% of Ti^{4+} and Co^{2+} ions incorporated in the grown crystals (run 16) correspond to ca. 0.5 mol of each ion and the formula unit is $\text{BaFe}_{11}\text{Ti}_{0.5}\text{Co}_{0.5}\text{O}_{19}$. The spin moment of Ti^{4+} is zero and

Table 2 Magnetic properties of minute $\text{BaFe}_{12}\text{O}_{19}$ crystals containing small amounts of Ti^{4+} and Co^{2+} ions; H_c = coercivity, M_s = saturation magnetization, M_r = remanence

run	magnetic properties		
	H_c/Oe	$M_s/\text{emu g}^{-1}$	$M_r/\text{emu g}^{-1}$
15	238.00	66.60	21.60
25	202.00	63.93	17.66
16	201.00	62.80	18.00
23	217.00	63.63	41.83
19	280.00	64.20	27.40
26	235.00	63.98	21.62
20	217.00	64.00	21.00
18	169.00	63.90	15.34

that of Co^{2+} ion is $3.7 \mu_{\text{B}}$ (0 K). Assuming that Ti^{4+} and Co^{2+} ions occupy 2b and $4f_{\text{VI}}$ crystalline sites with equal probability, we can consider the following three cases for the saturation moment of $\text{BaFe}_{11}\text{Ti}_{0.5}\text{Co}_{0.5}\text{O}_{19}$.

(1) Both Ti^{4+} and Co^{2+} ions enter into only the one side of the upward (2b) spin sites or downward ($4f_{\text{VI}}$) spin sites. In such a case, by simple arithmetic, the saturation magnetic moment, μ_s , per formula unit becomes considerably larger or smaller than $20 \mu_{\text{B}}$.

(2) Either of the Ti^{4+} and Co^{2+} enter into one side of the upward or the downward spin sites and the other enters into the other site. This results in μ_s larger than $20 \mu_{\text{B}}$.

(3) Some of the Ti^{4+} and Co^{2+} ions enter separately into the respective upward and downward spin sites. In such a case, μ_s becomes somewhat smaller than or equal to $20 \mu_{\text{B}}$.

Since, in the present study, the saturation magnetization decreased slightly with an increase of Ti^{4+} and Co^{2+} content and so both cases (1) and (2) can be discounted. Accordingly, case (3) is found to be valid. The saturation moment μ_s per formula unit $\text{BaFe}_{11}\text{Ti}_{0.5}\text{Co}_{0.5}\text{O}_{19}$ becomes:

$$\mu_{s,\text{calc}} = (20 - 1.26x)\mu_{\text{B}} \quad (2)$$

In the present study, the relation between the saturation magnetization, M_s , and the amounts, x , of Ti^{4+} and Co^{2+} ions in the crystals can be expressed by a linear relationship as;

$$M_s = (64.52 - 1.82x)\text{emu g}^{-1} \quad (3)$$

Moreover, the relation between M_s and the saturation magnetic moment per molecule, μ_s , can also be expressed by the following equation;

$$M_s = (\mu_{s,\text{ex}}\mu_{\text{B}}N_{\text{A}}/M_{\text{W}})\text{emu g}^{-1} \quad (4)$$

Where, N_{A} is Avogadro's number (6.02×10^{23}), μ_{B} is the Bohr magneton, 9.28×10^{-2} , and M_{W} is the molecular mass (1111.53).

Combining eqn. (3) and (4), leads to eqn. (5);

$$\mu_{s,\text{ex}} = (12.82 - 0.36x)\mu_{\text{B}} \quad (5)$$

Considering a constant, $C = 0.641 = 12.82/20$, reflecting the decrease in μ_s with increasing temperature, the relation of $\mu_{s,\text{calc}}$ vs. x at room temperature is:

$$\mu_{s,\text{calc}} = (12.82 - 0.81x)\mu_{\text{B}} \quad (6)$$

Comparing $\mu_{s,\text{ex}}$ deduced from the experimental data in eqn. (5) and $\mu_{s,\text{calc}}$ calculated with theoretical values in eqn. (6), it can be seen that the former, $\mu_{s,\text{ex}}$, has a smaller dependence upon the degree of substitution, x , of Ti^{4+} and Co^{2+} ions than the latter, $\mu_{s,\text{calc}}$.

It is also known that magnetic properties, such as coercivity, saturation magnetization and remanence, of crystals are noticeably influenced by vacancies, dislocations, irregular crystal surfaces and impurities, and that magnetocrystalline anisotropy depends on the shape and size of crystals.

Assuming the classical Stoner–Wohlfarth equation (coherent reversal) for a random particle assembly, the coercivity, H_c , for the barium ferrite, $\text{BaFe}_{12-2x}\text{Ti}_x\text{Co}_x\text{O}_{19}$, can be expressed by

$$H_c = 0.48 [(K_1/M_s) - N_d M_s] \quad (7)$$

where, C is a constant, K_1 is the uniaxial magnetocrystalline anisotropy constant, M_s is the saturation magnetization and N_d is the demagnetizing coefficient relating to the shape anisotropy.^{18,19} In the present study, the variation of M_s with the degree of substitution x is very small; furthermore, N_d for barium ferrite lies within a small range.^{4,15} Therefore, it can be considered that the decrease of H_c which occurs with increased degree of substitution x increases mainly through the anisotropy, K_1 . The origin of the uniaxial magnetocrystalline anisotropy of $\text{BaFe}_{12}\text{O}_{19}$ is largely dependent on the single-

ion anisotropy of the Fe^{3+} ions at the trigonal 2b and octahedral $4f_{V1}$ sites belonging to the R block.

Thus, when Fe^{3+} ions at these sites are replaced by other cations, it will be expected that the exchange interactions between two adjacent $4f_{V1}$ ions and the 2b ions are completely destroyed, and that the anisotropic magnetic properties of $\text{BaFe}_{12}\text{O}_{19}$ are significantly affected. As a result, this leads to a decrease of the coercivity. Accordingly, in the present study, we conjecture that the decrease in coercivity of grown crystals with increase of Ti^{4+} and Co^{2+} content is caused by the contribution of the magnetocrystalline anisotropy of Co^{2+} ions at the 2b sites.

Conclusions

Growth of minute single crystals of barium hexaferrite was carried out from high-temperature solutions of the $\text{Na}_2\text{O}-\text{B}_2\text{O}_3$ system containing small amounts of TiO_2 and CoO .

1. Optimum conditions to grow monosized minute $\text{BaFe}_{12}\text{O}_{19}$ single crystals with high quality are as follows: soaking temperature, 1200°C ; soaking time, 20 h; cooling rate, 4°C ; solvent, 10 mass% $\text{Na}_2\text{O}+5$ mass% B_2O_3 ; solute, $\text{BaO}+6\text{Fe}_2\text{O}_3$, 85 mass%; dopants, TiO_2 and CoO , <3 mass%.

2. Grown crystals show morphological evolution from hexagonal dipyramidal, truncated by $\{0001\}$, to hexagonal platy crystals as crystals grow larger. However, no morphological evolution was observed with the dopants TiO_2 and CoO .

3. A tendency was noted that yields and the size of $\text{BaFe}_{12}\text{O}_{19}$ crystals grown decreased with increasing TiO_2 and CoO dopant concentration; this effect was more marked with TiO_2 .

4. Lattice parameters a and c of the minute $\text{BaFe}_{12}\text{O}_{19}$ crystals decreased with an increase in TiO_2 and CoO content.

5. The coercivity of the crystals decreased with an increase of TiO_2 and CoO content, whereas reduction of remanence and saturation magnetization was much less significant. The

effect of Co^{2+} ion in diminution of the coercivity was larger than that of Ti^{4+} . It appears that the decrease of the coercivity of the grown crystals is associated with the contribution of magnetocrystalline anisotropy of Co^{2+} ions at the 2b sites.

References

- 1 T. Fujiwara, *IEEE Trans. Magn.*, 1985, **21**, 1480.
- 2 D. E. Speliotis, *IEEE Trans. Magn.*, 1990, **26**, 141.
- 3 J. Smit and H. P. Wijn, *Ferrites*, Philips Technical Library, International edn., 1965, pp. 172–211.
- 4 O. Kubo, T. Ido and H. Yokoyama, *IEEE Trans. Magn.*, 1982, **18**, 1120.
- 5 M. Pernet, X. Obradors, M. Vallet, T. Hernandez and P. Germi, *IEEE Trans. Magn.*, 1988, **24**, 1898.
- 6 P. W. McMillan, *Glass Ceramics*, Academic, London, 2nd edn. 1979, pp. 74–76.
- 7 D. Elwell and H. J. Scheel, *Crystal Growth from High Temperature Solutions*, Academic, London, 1975, pp. 278.
- 8 K. Watanabe, *J. Crystal Growth*, 1993, **131**, 181.
- 9 K. Watanabe, *J. Crystal Growth*, 1996, **169**, 509.
- 10 R. Collongues, D. Gourier, A. Kahn-Harari, A. M. Lejus, J. Thery and D. Vivien, *Annu. Rev. Mater. Sci.*, 1990, **20**, 51.
- 11 D. J. DeBitetto, *J. Appl. Phys.*, 1964, **35**, 3482.
- 12 V. F. Belov, T. A. Khimich, M. N. Shipko, I. S. Zheludev, E. V. Korneev and N. S. Ovanesyan, *Sov. Phys. JETP*, 1973, **37**, 1089.
- 13 H. Yamada, M. Takano, M. Kiyama, T. Takada, T. Shinjo and K. Watanabe, *Adv. Ceram.*, 1985, **16**, 169.
- 14 F. Chou, X. Feng, J. Li and Y. Liu, *J. Appl. Phys.*, 1987, **61**, 3881.
- 15 X. Z. Zhou, A. H. Morrish, Z. W. Li and Y. K. Hong, *IEEE Trans. Magn.*, 1991, **27**, 4654.
- 16 R. D. Shannon, *Acta Crystallogr., Sect. A*, 1976, **32**, 751.
- 17 D. H. Han, Z. Yang, H. X. Zeng, X. Z. Zhou and A. H. Morrish, *J. Magn. Magn. Mater.*, 1994, **137**, 191.
- 18 A. R. Corradi, D. E. Speliotis, A. H. Morrish, Q. A. Pankhurst, X. Z. Zhou, G. Bottoni, D. Candolfo, A. Cecchetti and F. Masoli, *IEEE Trans. Magn.*, 1988, **24**, 2862.
- 19 R. S. Tebble and D. J. Craik, *Magnetic Materials*, Wiley, London, 1969, pp. 447–455.

Paper 7/02126G; Received 27th March, 1997